

## Temperature and ion irradiation dependence of magnetic domains and microstructure in Co/Pt multilayers

G. J. Kusinski<sup>a),b)</sup> G. Thomas,<sup>b)</sup> G. Denbeaux, and K. M. Krishnan  
*Materials Sciences Division, Lawrence Berkeley National Laboratory, Berkeley, California 94720*

B. D. Terris  
*IBM Almaden Research Center, 650 Harry Road, San Jose, California 95120*

Microstructure and magnetic properties of Co/Pt multilayers with perpendicular anisotropy were studied as a function of growth temperature ( $T_G$ ) and ion irradiation. With increased  $T_G$ , larger columnar grain size and an improved  $\langle 111 \rangle$  texture were observed. Up to a critical temperature ( $T_{crit}$ ), a monotonic increase in coercivity ( $H_C$ ) with  $T_G$  was measured, followed by a decrease in  $H_C$  with further increase in  $T_G$ . Magnetic domains of films grown below  $T_{crit}$  were irregular, with their submicron size decreasing gradually with increasing  $T_G$ . Films grown at  $390^\circ\text{C} > T_{crit}$  had fine domains on the sub-100 nm length scale. Both  $H_C$  and domain size were reduced after the multilayers were exposed. © 2002 American Institute of Physics. [DOI: 10.1063/1.1452230]

Magnetic multilayers (MLs) composed of modulated ferromagnetic–nonmagnetic layers have attracted much attention in recent years. In particular, Co/Pt MLs,<sup>1–3</sup> with large perpendicular magnetic anisotropy (PMA) and high coercivity have been proposed as future magnetic media in Terabit/in<sup>2</sup> magnetic recording systems.<sup>4</sup> Moreover, ion-beam irradiation has been shown to modify the magnetic properties in such MLs by effectively reducing PMA.<sup>5–7</sup> Hence, local patterning of magnetic properties can be achieved by application of spatially varying irradiation

dose.<sup>8,9</sup> Understanding the magnetic domain structure in such films is important from a technological as well as a fundamental perspective. In this article, the influence of growth temperature<sup>10</sup> and ion-beam irradiation on magnetic properties and, in particular, on the domain structure and coercivity,  $H_C$ , is discussed.

For the specific experiments discussed here, Co/Pt MLs with the following structure: /20 nm Pt seed/10 × (0.3 nm Co/1 nm Pt)/1 nm Pt cap layer/, were fabricated by electron-beam evaporation.<sup>10</sup> For the purpose of transmis-

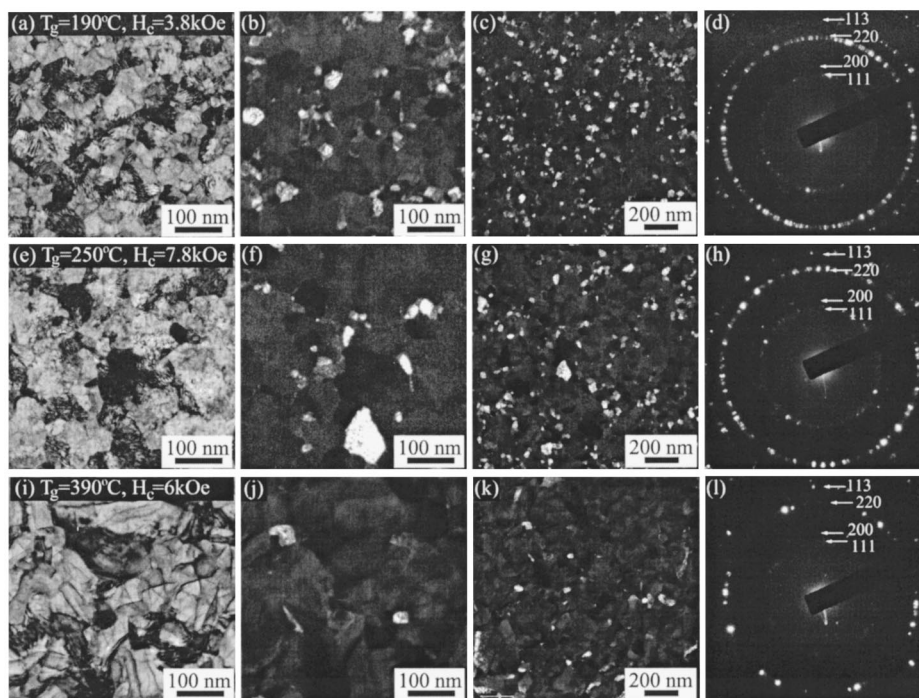


FIG. 1. Plan-view BF TEM images, SAD patterns and (111)DF images of the Co/Pt MLs grown at  $T_G = 190^\circ\text{C}$ ,  $T_G = 250^\circ\text{C}$ , and  $T_G = 390^\circ\text{C}$ , displayed in rows. All SADs were collected with a  $5\ \mu\text{m}$  aperture.

<sup>a)</sup>Electronic mail: kusinski@alum.calberkeley.org

<sup>b)</sup>Also at: Department of Materials Science and Engineering, University of California, Berkeley, CA 94720.

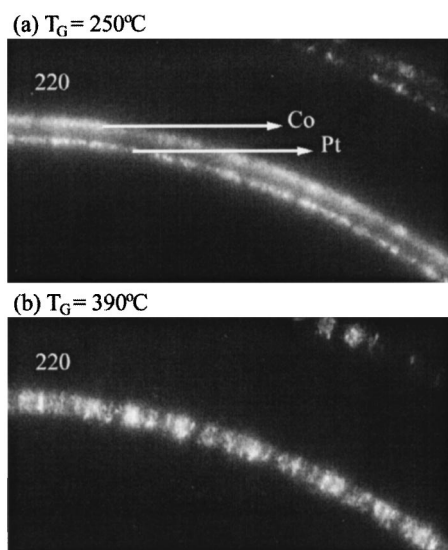


FIG. 2. Enlarged sections of SAD patterns. (a)  $T_G = 250^\circ\text{C}$  and (b)  $T_G = 390^\circ\text{C}$ .

sion electron microscopy (TEM) and magnetic transmission x-ray microscopy (MTXM) imaging, MLs were deposited on electron transparent  $\text{Si}_3\text{N}_4$  windows. For all samples discussed in this article, both the 20 nm Pt seed layer, and the ML stack were evaporated at roughly the same growth temperature,  $T_G$ , ranging between 200 and  $390^\circ\text{C}$ . In addition, samples were exposed to 700 keV  $\text{N}^+$  ion irradiation, from a NEC 3UH Pelletron accelerator. Magnetic hysteresis measurements were performed using magneto-optical Kerr effect (MOKE) techniques.

The microstructure of all samples was evaluated by TEM (using a Philips CM200FEG and a JEOL 3010), utilizing bright field-(BF), dark field-(DF), and high resolution-(HRTEM) imaging, and selected area diffraction (SAD). High resolution magnetic imaging was performed with a magnetic transmission x-ray microscope,<sup>11–13</sup> to study the magnetic domain structure as a function of growth temperature and ion irradiation dose with a 25 nm spatial resolution.<sup>14</sup>

As depicted in Fig. 1, all of the investigated samples were polycrystalline with an average grain size increasing with  $T_G$ . The SAD patterns, Figs. 1(d), 1(h), and 1(l), showed a typical ring spacing associated with polycrystalline face-centered-cubic Pt structure. For all samples, (111) and (002) rings were weak, but not zero, and the (022) ring was the strongest. This implies strong out-of-plane  $\langle 111 \rangle$  texture,<sup>15</sup> with only some grains oriented randomly, contributing to (111) and (002) rings. The SAD patterns from larger areas show a uniform intensity distribution around all rings indicating random in-plane orientation and only out-of-plane  $\langle 111 \rangle$  texture.

Figures 1(b), 1(f), and 1(d) are (111) DF images showing only the grains without the  $\langle 111 \rangle$  texture and Figs. 2(c), 2(g), and 2(k) are respective lower magnification images showing the distribution of such grains. As presented, samples grown at the low temperature of  $190^\circ\text{C}$ , Figs. 2(b) and 2(c), had a large number of uniformly distributed grains lacking the  $\langle 111 \rangle$  texture. With increasing  $T_G$ , the number of such mis-

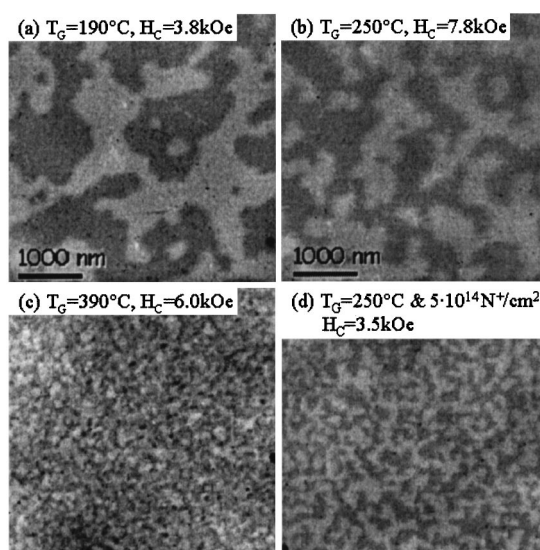


FIG. 3. MTXM images of samples grown at different  $T_G$ : (a)  $190^\circ\text{C}$ , (b)  $250^\circ\text{C}$ , (c)  $390^\circ\text{C}$ , and (d) same sample as in image (b) but irradiated with 700 keV  $5 \times 10^{14} \text{N}^+/\text{cm}^2$ .

oriented grains decreased. For the  $T_G = 250^\circ\text{C}$  sample, Figs. 2(f) and 2(g), the majority of the misoriented grains were smaller than the average grain size, although a few large misoriented grains were also found. For samples grown at  $390^\circ\text{C}$ , a good  $\langle 111 \rangle$  texture was observed, with only very few grains lacking the  $\langle 111 \rangle$  texture, as shown in Figs. 2(j) and 2(k). Moreover, such misoriented grains were much smaller than the  $\langle 111 \rangle$  textured grains.

Figures 2(a) and 2(b) show enlarged sections of SAD patterns for samples grown at 250 and  $390^\circ\text{C}$ , respectively. For lower  $T_G$  samples,  $190^\circ\text{C}$  (not presented) and  $250^\circ\text{C}$ , all diffraction rings were split indicating two distinctive lattice parameters for the Co and Pt layers. The relative ratio of Co to Pt rings was 0.97, indicating highly strained Co layers. This splitting explains a fine Moiré fringe contrast, visible in some of the grains for 190 and  $250^\circ\text{C}$  films, Figs. 2(a) and 2(e). However, the intensity in the two subrings had the same radial distribution, indicative of columnar growth extending throughout the thickness of the multilayer stack, with the grain size determined by the seed layer. This was also confirmed by HRTEM. For samples grown above a critical transition temperature,  $T_{\text{crit}}$ , the ring splitting attributed to two separate Pt and Co parameters was not detectable, as shown by one broad ring in Fig. 2(b), indicating a continuous gradient in lattice parameter between that of strained Co (measured for 190 and  $250^\circ\text{C}$ ) and Pt.

In addition to effecting the grain size and the  $\langle 111 \rangle$  texture,  $T_G$  is also known to influence magnetic properties (i.e.,  $H_C$ , domain size).<sup>16</sup> As shown in Fig. 3, MTXM was used to investigate the magnetic domain size, and MOKE was used to measure  $H_C$ . It was reported earlier that  $H_C$  of the Co/Pt MLs increases almost linearly with increasing  $T_G$ .<sup>10,17</sup> Moreover, Weller *et al.*<sup>10</sup> showed that when  $T_G$  is increased beyond  $T_{\text{crit}}$  a decrease in  $H_C$  is observed.

For samples grown below  $T_{\text{crit}}$ , square loops were observed with a high hysteresis slope. The increase in  $H_C$  in this temperature regime was associated with small shearing

of the loops, seen as a small decrease in the hysteresis slope. The increase in  $H_C$  correlates with an observed increase in grain size and improvement of the  $\langle 111 \rangle$  texture. Similar values of  $H_C$  and nucleation,  $H_N$ , were measured, indicating a magnetic reversal, which is communicated throughout the film via strong exchange coupling between grains. In agreement, the MTXM imaging found large irregularly shaped submicrometer magnetic domains. As shown, Figs. 3(a) and 3(b), the size of the observed domains was found to decrease with increasing  $T_G$ , consistent with the increase in  $H_C$ .

On the other hand, for samples grown above  $T_{crit}$ , the hysteresis loops were significantly sheared, indicating reversal over a broad range of  $H_A$ . This suggests magnetic clusters that reverse rather independently of their neighbors over a range of  $H_A$ , implying an exchange de-coupled granular system. For these samples, a very fine domain structure, comprised of individual grains or small clusters of similarly oriented grains, with length scales below 100 nm was observed as shown in Fig. 3(c) for sample  $T_G = 390^\circ\text{C} > T_{crit}$ . TEM analysis of the  $T_G = 390^\circ\text{C}$  sample showed one set of CoPt rings indicating diffused interfaces, which correlates with the observed reduction in PMA measured as lower  $H_C$ . Moreover, energy filtered TEM revealed Co depleted, Pt rich columnar boundaries in samples grown above  $T_{crit}$ . This can explain magnetic measurements, which indicate grain decoupling, and may help explain the small size of the observed domains.

As reported earlier,<sup>7</sup> ion irradiation can be used to reduce the perpendicular anisotropy of these Co/Pt multilayers. Doses of 700 keV  $\text{N}^+$  as low as  $10^{14} \text{N}^+/\text{cm}^2$  reduce  $H_C$  without, however, effecting the square loop shape. A substantial decrease in the perpendicular remanence is observed for doses above  $\sim 10^{15} \text{N}^+/\text{cm}^2$ . When the dose is increased further (beyond  $3-4 \times 10^{15} \text{N}^+/\text{cm}^2$ ), the transition from out-of-plane to in-plane easy axis orientation occurs. These effects are associated with a gradual decrease in the PMA.

Figure 3(d) shows an MTXM, domain image of the sample grown at  $T_G = 250^\circ\text{C}$  and irradiated with 700 keV  $5 \times 10^{14} \text{N}^+/\text{cm}^2$ , a dose sufficient to reduce  $H_{C\perp}$  by half, to approximately 3.5 kOe. Comparing Figs. 3(d) and 3(b), which shows magnetic domains in the as-grown state, a substantial decrease in domain size after ion irradiation is evident. However, the domains still had similar irregular appearance but a smaller feature size. A similar decrease in domain size upon ion irradiation was found for all the samples, with larger doses yielding a smaller domain size. The TEM investigations of the ion irradiated samples revealed no noticeable grain size changes from the as-grown samples even at the doses of  $5 \times 10^{16} \text{N}^+/\text{cm}^2$ , which are  $\sim 10$  times larger than those needed to fully reduce PMA and render in-plane magnetization. For these MLs, the ion induced decrease in  $H_C$  is associated with the reduction in the PMA.

Moreover, combining and re-emphasizing the results presented in Figs. 3(a), 3(b), and 3(d) an important conclusion is made. The domain sizes,  $D$ , are not directly determined by  $H_C$ , and are governed in a complex way by both the PMA and the microstructure. As shown,  $D(190^\circ\text{C}, H_C = 3.8 \text{ kOe}) > D(250^\circ\text{C}, H_C = 7.8 \text{ kOe})$  yet  $> D(250^\circ\text{C}$  and  $5 \times 10^{14} \text{N}^+/\text{cm}^2, H_C = 3.5 \text{ kOe})$ . When  $T_G$  is increased

from  $190^\circ\text{C}$ —Fig. 3(a) to  $250^\circ\text{C}$ —Fig. 3(b),  $H_C$  increases and domain size decreases. The increase in  $T_G$  results in improved  $\langle 111 \rangle$  texture what gives increased anisotropy resulting in increase of  $H_C$  from 3.8 to 7.8 kOe, corresponding to smaller  $D$ . When the  $T_G = 250^\circ\text{C}$  sample was then irradiated, which reduced  $H_C$  back down to 3.5 kOe, the smallest domain size was observed [Fig. 3(d)]. In the latter step, however, the grain structure is not changed, and only the PMA is reduced due to local intermixing of the MLs. Hence, the ion irradiation reduces the domain size, similar to the increase in  $T_G$  in the high temperature regime, above  $T_{crit}$ .

To summarize, changes in the domain structure with processing parameters, i.e.,  $T_G$  and  $\text{N}^+$  ion dose, were investigated. With increase in  $T_G$  up to  $T_{crit}$ , an increase in grain size and an improved  $\langle 111 \rangle$  texture were found, both contributing to increase in  $H_C$ . Moreover, a decrease in the domain size was observed. For MLs grown at  $T_G = 390^\circ\text{C} > T_{crit}$ , a decrease in  $H_C$  was measured, and small magnetically decoupled domains, with size about the grain size, were observed. This correlates well with Co depletion at the column grain boundaries and diffused Co/Pt interfaces. The latter one is known to reduce the PMA and, hence, reduce  $H_C$ .

One of the authors (G. K.) acknowledges financial support through the “IBM Research Fellowship.” The authors thank J. E. E. Baglin and A. Kellock for ion radiation support. Work at NCEM/LBNL was supported by the U.S. Department of Energy under Contract No. DE-AC03-76SF00098.

<sup>1</sup>P. F. Garcia, J. Appl. Phys. **63**, 5066 (1988).

<sup>2</sup>Z. G. Li, P. F. Garcia, and Y. Cheng, J. Appl. Phys. **73**, 2433 (1993).

<sup>3</sup>D. Weller, R. F. C. Farrow, R. F. Marks, G. R. Harp, H. Notarys, and G. Gorman, Mater. Res. Soc. Symp. Proc. **313**, 791 (1993).

<sup>4</sup>R. Wood, IEEE Trans. Magn. **36**, 36 (2000).

<sup>5</sup>C. Chappert, H. Bernas, J. Ferre, V. Kottler, J.-P. Jamet, Y. Chen, E. Cambriil, T. Devolder, F. Rousseaux, V. Mathet, and H. Launois, Science **280**, 1919 (1998).

<sup>6</sup>J. Ferre, C. Chappert, H. Bernas, J.-P. Jamet, P. Meyer, O. Kaitasov, S. Lemerle, V. Mathet, F. Rousseaux, and H. Launois, J. Magn. Magn. Mater. **191**, 198 (1999).

<sup>7</sup>D. Weller, J. E. E. Baglin, A. J. Kellock, K. A. Hannibal, M. F. Toney, G. Kusinski, S. Lang, L. Folks, M. E. Best, and B. D. Terris, J. Appl. Phys. **87**, 5768 (2000).

<sup>8</sup>T. Devolder, C. Chappert, Y. Chen, E. Cambriil, H. Bernas, J. P. Jamet, and J. Ferre, Appl. Phys. Lett. **74**, 3383 (1999).

<sup>9</sup>B. D. Terris, L. Folks, D. Weller, J. E. E. Baglin, A. J. Kellock, H. Rothuizen, and P. Vettiger, Appl. Phys. Lett. **75**, 403 (1999).

<sup>10</sup>D. Weller, L. Folks, M. Best, E. E. Fullerton, B. D. Terris, G. J. Kusinski, K. M. Krishnan, and G. Thomas, J. Appl. Phys. **89**, 7525 (2001).

<sup>11</sup>P. Fischer, G. Schutz, G. Schmahl, P. Guttman, and D. Raasch, Z. Phys. B: Condens. Matter **101**, 313 (1996).

<sup>12</sup>The MTXM is built and operated by the Center for X-ray Optics at the beam line 6.1.2 of the Advanced Light Source at the Lawrence Berkeley National Laboratory.

<sup>13</sup>G. Denbeaux, P. Fischer, G. Kusinski, M. L. Gros, A. Pearson, and D. Attwood, IEEE Trans. Magn. **37**, 2764 (2001).

<sup>14</sup>G. J. Kusinski, K. M. Krishnan, G. Denbeaux, G. Thomas, D. Weller, and B. D. Terris, Appl. Phys. Lett. **79**, 2211 (2001).

<sup>15</sup>D. B. Williams and C. B. Carter, *Transmission Electron Microscopy: A Textbook for Materials Science* (Plenum, New York, 1996).

<sup>16</sup>G. J. Kusinski, K. M. Krishnan, G. Thomas, and E. C. Nelson, J. Appl. Phys. **87**, 6376 (2000).

<sup>17</sup>S. Shiomi, T. Nishimura, T. Kobayashi, and M. Masuda, Jpn. J. Appl. Phys., Part 2 **32**, L495 (1993).